Field-induced quantum soliton lattice in a frustrated two-leg spin-1/2 ladder

Casola, Francesco; Shiroka, Toni; Feiguin, Adrian; Wang, Shuang; Grbić, Mihael Srđan; Horvatić, Mladen; Kramer, Steffen; Mukhopadhyay, Sutirtha; Conder, K.; Berthier, Claude; ...

Source / Izvornik: **Physical Review Letters, 2013, 110**

Journal article, Published version
Rad u časopisu, Objavljena verzija rada (izdavačev PDF)

https://doi.org/10.1103/PhysRevLett.110.187201

Permanent link / Trajna poveznica: https://urn.nsk.hr/urn:nbn:hr:217:198385

Field-Induced Quantum Soliton Lattice in a Frustrated Two-Leg Spin-1/2 Ladder

F. Casola,[1,2,*] T. Shiroka,[1,2] A. Feiguin,[3] S. Wang,[4,5] M. S. Grbić,[6,7] M. Horvatić,[7] S. Krämer,[7] S. Mukhopadhyay,[7] K. Conder,[4] C. Berthier,[7] H.-R. Ott,[1,2] H. M. Rønnow,[5] Ch. Rüegg,[8,9] and J. Mesot[1,2]

[1]*Laboratorium für Festkörperphysik, ETH Hönggerberg, CH-8093 Zürich, Switzerland*
[2]*Paul Scherrer Institut, CH-5232 Villigen PSI, Switzerland*
[3]*Department of Physics, Northeastern University, Boston, Massachusetts 02115, USA*
[4]*Laboratory for Developments and Methods, Paul Scherrer Institut, CH-5232 Villigen PSI, Switzerland*
[5]*Laboratory for Quantum Magnetism, Ecole Polytechnique Fédérale de Lausanne, CH-1015 Lausanne, Switzerland*
[6]*Department of Physics, Faculty of Science, University of Zagreb, P.O. Box 331, HR-10002 Zagreb, Croatia*
[7]*Laboratoire National des Champs Magnétiques Intenses, LNCMI-CNRS (UPR3228), UJF, UPS and INSA, B.P. 166, 38042 Grenoble Cedex 9, France*
[8]*Laboratory for Neutron Scattering, Paul Scherrer Institute, CH-5232 Villigen PSI, Switzerland*
[9]*DPMC-MaNEP, University of Geneva, CH-1211 Geneva, Switzerland*

(Received 27 November 2012; published 30 April 2013)

Based on high-field ^{31}P nuclear magnetic resonance experiments and accompanying numerical calculations, it is argued that in the frustrated $S = 1/2$ ladder compound $BiCu_2PO_6$ a field-induced *soliton* lattice develops above a critical field of $\mu_0 H_{c1} = 20.96(7)$ T. Solitons result from the fractionalization of the $S = 1$, bosonlike triplet excitations, which in other quantum antiferromagnets are commonly known to experience Bose-Einstein condensation or to crystallize in a superstructure. Unlike in spin-Peierls systems, these field-induced quantum domain walls do not arise from a state with broken translational symmetry and are triggered exclusively by magnetic frustration. Our model predicts yet another second-order phase transition at $H_{c2} > H_{c1}$, driven by soliton-soliton interactions, most likely corresponding to the one observed in recent magnetocaloric and other bulk measurements.

DOI: 10.1103/PhysRevLett.110.187201 PACS numbers: 75.10.Pq, 75.10.Jm, 75.40.Cx, 76.60.−k

Most of the current interest in field-induced (FI) phases of quantum antiferromagnets is based on the close analogy between the low-energy physics of these spin systems and the physics of bosons with a contact (hard-core-like) repulsion [1–4]. In this context, FI phases can be studied by identifying the magnetic field as an effective chemical potential [1] and by noting the equivalence of the universality classes of the quantum phase transition (QPT) of the spin and particle problem, respectively [5,6].

Paradigmatic in this context are spin-1/2 ($S = 1/2$) antiferromagnets with a nonmagnetic singlet ground state and bosonlike $S = 1$ triplet excitations, known as *triplons* [2,7]. Upon the application of a critical field H_{c1}, whose Zeeman energy equals the zero-field energy gap $\Delta(H = 0)$, the triplons soften and can experience a Bose-Einstein condensation (BEC) at low temperatures [2,7]. The off-diagonal long-range order (LRO) of the BEC is reflected as a magnetic order of the spin component transverse to the applied field [6]. Frustrating next-nearest neighbor (NNN) spin-exchange interactions are expected to notably affect the universality of the QPT. It has been shown, both theoretically [3,8] and experimentally [3,4], that frustration leads to a reduction of the triplon hopping energy and to a concomitant increase of their mutual interactions. Hence, triplons can crystallize into incompressible phases with broken translational symmetry, as observed, e.g., in the 2D magnetic insulator $SrCu_2(BO_3)_2$ [4].

Based on results of nuclear magnetic resonance (NMR) experiments and model calculations presented below, we argue that in the $S = 1/2$ ladder compound $BiCu_2PO_6$, geometric frustration does not merely shift the propagation vector of the transverse LRO to some incommensurate (IC) location in reciprocal space, as expected from BEC theories [9]. Neither does it lead to a spin-density wave, as expected in materials with a triplon crystallization in superstructures [3]. Instead, we find that triplons fractionalize, and the magnetization process at $H \geq H_{c1}$ is to be viewed in terms of $S = 1/2$ quantum domain walls, called *solitons*, introduced as basic excitations, e.g., in the context of quasi-1D frustrated spin chains [10,11]. Upon partially replacing $S = 1/2$ Cu by $S = 0$ Zn atoms, the critical field increases, but the ordered phase persists.

In $BiCu_2PO_6$, the ladders run along the b axis of the crystal structure [12,13], with rung and leg exchange $J_\perp$ and J_1, respectively. The inequivalence of the Cu^{2+} sites allows the NNN exchange constants to alternate in magnitude [14] [J_2 and $\tilde{J}_2$ in the inset in Fig. 1(c)]. Residual interladder interactions are expected along the c direction, while PO_4 tetrahedra act as nonmagnetic spacers between different bc planes [14–16].

Selected ^{31}P NMR data obtained from $2 \times 2 \times 2$ mm^3 single crystals [13] of $Bi(Cu_{1-x}Zn_x)_2PO_6$ in magnetic fields up to 31 T, a range currently not accessible to, e.g., neutron diffraction experiments, are shown in Fig. 1(a) for $x = 0$ and $x = 0.01$ [17]. The field was applied along the b

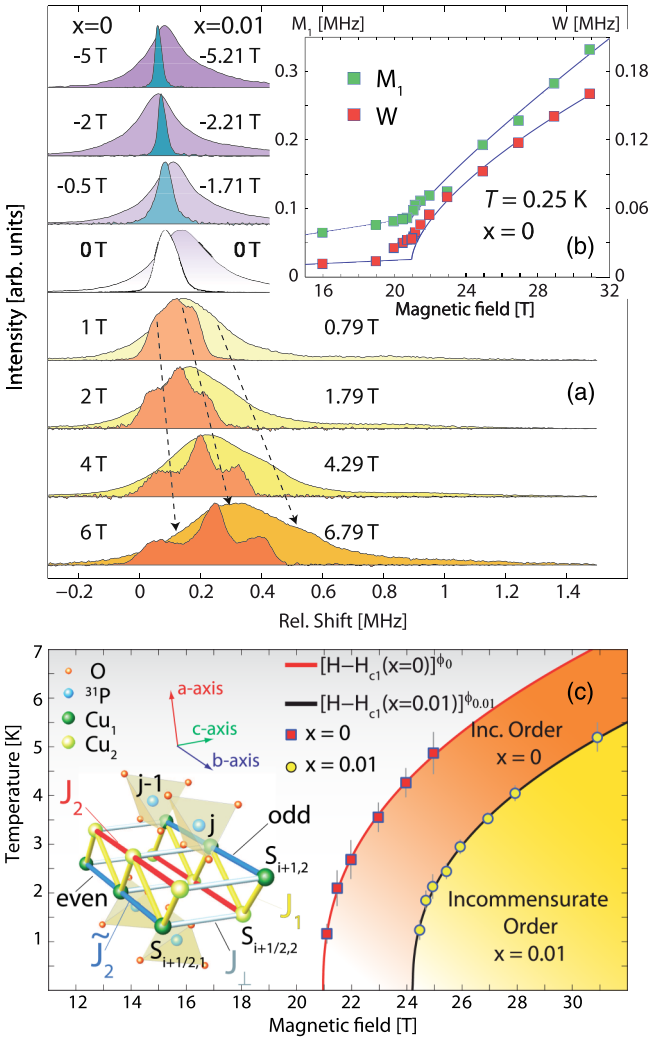

FIG. 1 (color online). (a) NMR lines $I(f)$ in the field-induced phase of $Bi(Cu_{1-x}Zn_x)_2PO_6$. The ^{31}P NMR line shapes of $x = 0$, ($x = 0.01$) $Bi(Cu_{1-x}Zn_x)_2PO_6$ taken at 0.25 K (1.4 K) are placed in the foreground (background) with the corresponding magnetic field values on the left (right) relative to the critical field of 20.96(7) T [24.21(9) T]. The frequency scale is relative to the Larmor frequency. Arrows show the position of the three weakly resolved peaks for $x = 0.01$. (b) Field dependence of the first moment (M_1) and the square root of the second moment (W) of the spectra, with lines to guide the eye. (c) FI ordered phases, as determined from peaks in the $T_1^{-1}(T, H)$ relaxation data (see the text for details). A structural unit of $BiCu_2PO_6$ is shown in the lower left corner. Even (odd) refers to the parity of the ith Cu site.

axis with $\pm 3°$ uncertainty, and the covered temperature range was between 0.25 and 20 K. We studied the onset of the FI phases appearing at the critical field $H_{c1}(x, T)$ for the two quoted x values. For $H < H_{c1}$, the $x = 0$ system is disordered due to quantum fluctuations. The uniform local magnetization results in the same sharp NMR resonance for all the ^{31}P sites, broadened for the $x = 0.01$ sample due to Zn impurities. For $H > H_{c1}$, when the spin gap is closed, a triple-peak NMR line shape appears in both samples, well resolved in one and less distinct in the other, in accordance with the initial linewidths. These line shapes indicate a continuous distribution of local fields, suggestive of magnetic order with an *incommensurate* spin pattern [19]. Nonmagnetic Zn atoms create finite-length Cu ladders but do not seem to modify the type of order adopted for $x = 0$. The onset of LRO at $H_{c1}(x, T)$ is revealed by the strong increase with field of both the first moment M_1 and the square root of the second moment W of the line $I(f)$ [see Fig. 1(b)]. The normalized NMR line shape $I(f)$ is dictated by the distribution of $\gamma_P h_p(j)$, with $\gamma_P H$ the Larmor frequency and $h_p(j)$ the local field due to the ith Cu^{2+} ion at the jth ^{31}P nucleus along the b direction [see the inset in Fig. 1(c) for the notation]. The four ^{31}P sites in a unit cell are labeled by the index p. The local field can be written as $h_p(j) \simeq \sum_{l,\lambda} A_l^{\lambda,p}(S_{i+1,l}^{\lambda} - S_{i,l}^{\lambda}) + \sum_l A_l^b(S_{i+1,l}^b + S_{i,l}^b)$, where $\lambda = a, c$. The ladder leg is denoted by l, and the i values are integer multiples of $1/2$. The complete set of hyperfine couplings $A_l^{\lambda,p}$ to the electronic spin $\mathbf{S}_{i,l}$ of Cu^{2+} was obtained by fitting the rotation patterns of the maxima of the main and the impurity-induced satellite NMR lines for $x = 0.01$ [18,20]. Direct comparisons of spin-structure models with experimental lines and their moments [21] are thus possible.

The onset of magnetic order is also indicated by the nuclear relaxation rate $T_1^{-1}(T, H)$, whose (T, H) dependences are displayed in Fig. 2(a). For $H < H_{c1}$ and $x = 0$,

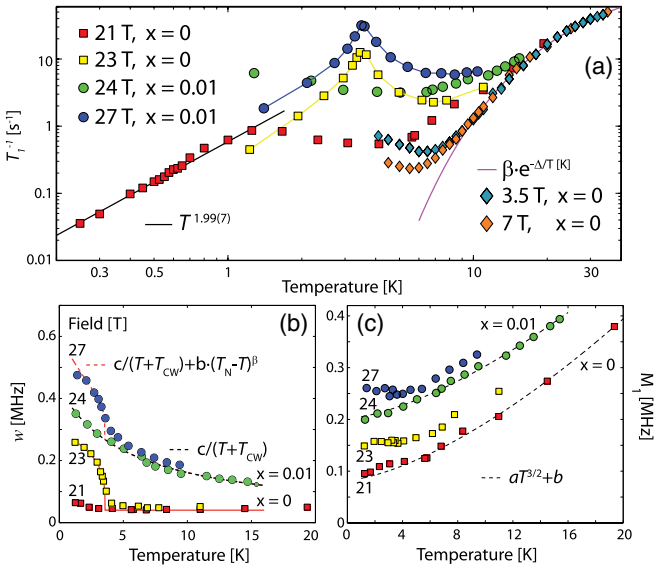

FIG. 2 (color online). (a) T dependence of T_1^{-1} for various representative fields and x values. The solid line for $T \geq 6$ K is a fit to $\exp(-\Delta/T)$, with $\Delta = 51.6(7)$ K. (b) T dependence of the NMR linewidths $w(T, H)$ at 1/4 of the line maxima for $x = 0$ and $x = 0.01$. The expression $c/(T + T_{CW})$ represents a Curie-Weiss law, while the power-law exponent of the order parameter [fitted by fixing T_N from Fig. 1(b)] was found to be $\beta = 0.31(6)$ for the $x = 0$ case. (c) T dependence of $M_1(T)$.

an activated behavior reflects the gap in the excitation spectrum [18]. The distinct upturn of T_1^{-1} below 10 K is reduced by the applied field. This can be related to residual impurity effects, as those occurring in gapped Haldane chains [22]. Clear maxima in $T_1^{-1}(T, H)$ are instead observed for both samples if $H > H_{c1}(x)$ [see Fig. 2(a)], serving to map the phase boundaries shown in Fig. 1(c). The data were fitted by $T_N \propto [H_c(x, T) - H_{c1}(x, 0)]^{\phi_x}$, resulting in $\phi_0 = 0.42(5)$, $\phi_{0.01} = 0.41(3)$ (i.e., unaltered), and $\mu_0 H_{c1}(0, 0) = 20.96(7)$ T, $\mu_0 H_{c1}(0.01, 0) = 24.21(9)$ T. The shift of $H_{c1}(x, 0)$ for $x = 0.01$, of about 3.2 T, can be ascribed to the random suppression of the spin degrees of freedom in the ladder [23]. The value of the exponent ϕ_0 is in good agreement with a recent mapping of the phase diagram using torque magnetometry at $T < 1$ K [24]. Note that ϕ_0 is notably different from $\phi_0 = 2/d$, expected for a d-dimensional FI BEC of triplet excitations. This difference may be caused by both anisotropy and frustration [2,25]. A **g**-tensor anisotropy can be ruled out by symmetry for $\mathbf{H} \parallel b$. Even so, we see that, for $H < H_{c1}$, both M_1 and W are nonzero and increase linearly with H, implying that both $S^b_{i,l}$ and $S^\lambda_{i,l} \neq 0$. This suggests the presence of anisotropic Dzyaloshinskii-Moriya (DM) interactions [14,26], which are allowed by crystal symmetry [14]. However, DM terms are expected to leave a residual spin gap even at $H_{c1}(0, 0)$ [8]. Our $T_1^{-1}(T, H_{c1})$ data, shown in Fig. 2(a), do not exhibit a corresponding activated but rather a polynomial T dependence down to $T_{\min} = 0.3$ K. This indicates that the effects of magnetic anisotropies on ϕ, although present, may appear [25] only when $[H_c(T) - H_{c1}(x, 0)] \leq T_{\min} k_B / g\mu_B \sim 0.25$ T. By varying the temperature at $H = H_{c1}$, we recover features consistent with those of quantum antiferromagnets with $S = 1$ excitations [27]: From the $x = 0$ data in Fig. 2(c), we see that $M_1(T)$, proportional to the uniform magnetization of the system [21], varies as $M_1(T) \propto T^{3/2}$ [27]. The linewidth $w(T)$, which we choose as a measure of the order parameter, is instead constant [Fig. 2(b)].

For $x = 0.01$, FI magnetic order is again revealed by monitoring the width $w(T, H)$, where a field-induced contribution is well visible above the Curie-Weiss-type broadening [see Fig. 2(b)]. FI magnetic order is absent in other disordered quasi-1D spin systems with incommensurate correlations [28,29]. Its stability in $Bi(Cu_{1-x}Zn_x)_2PO_6$ is likely to reveal important information on the nature of the FI order for $x = 0$ [28].

As outlined below, we use numerical tools to study the field-induced IC spin structure realized in $BiCu_2PO_6$ for $H \gtrsim H_{c1}$. We investigate the magnetization process of the ladder model with NNN exchange interactions proposed for $BiCu_2PO_6$ [14]. We show that it corresponds to the formation of solitons with effective spin $S = 1/2$, arising from the fractionalization of an FI static magnetic triplon. Our model also accounts for an additional QPT at $H > H_{c1}$, recently observed in experiments [16].

From a classical point of view, the natural state of frustrated 1D materials in a magnetic field is a canted spin helix [25,30]. In a quantum-mechanical treatment, a renormalization of both the pitch angle and the magnitude of the ordered moments is expected [31]. Since in $BiCu_2PO_6$ the geometrical frustration acts only along the ladder, we considered a tilted cone (i.e., helical) arrangement of the magnetic moments with $\mathbf{S}_{i,l} = \bar{R}_{\eta,\epsilon}(m_{l,\perp}\cos\theta_i, m_{l,\parallel}, m_{l,\perp}\sin\theta_i)$. The matrix $\bar{R}_{\eta,\epsilon}$ rotates the spin structure away from the applied-field axis b by a polar and an azimuthal angle (η, ϵ), while $\theta_i = qi$, with $\mathbf{q} \parallel b$ the propagation vector. Along the ladder rungs we chose the antiferromagnetic order $m_{1,\perp} = -m_{2,\perp}$. The resulting NMR lines, simulated for several η, ϵ, and q values, using the known hyperfine parameters, exhibit profiles as those in Fig. 3(b), in clear disagreement with experimental data. The experimental resolution was taken as the linewidth of $BiCu_2PO_6$ at 19 T.

In order to retain quantum effects in the model, we performed a density-matrix renormalization group (DMRG) analysis of the FI phase transition in a system

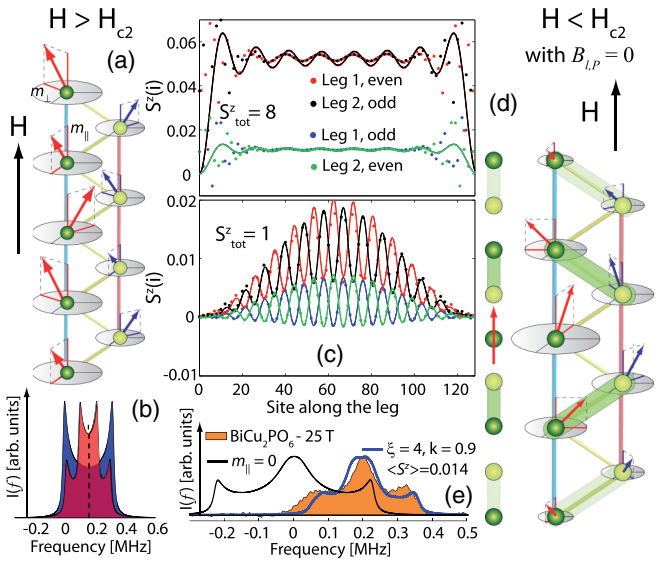

FIG. 3 (color online). (a) The untilted helix expected for $H > H_{c2}$. The gray circle is proportional to the magnitude of the moment. (b) Typical simulated $I(f)$ for a helical spin cone structure, where $q = q_1$ (background) or $q = 2q_1$ (foreground), with $q_1 = 0.5 \pm \delta$ ($\delta \approx 0.04$ and q is in reciprocal lattice units) and $\eta = 45°$. $m_\perp$ was taken such that the widths are comparable with the data in panel (e). (c) Points are $S^z(i)$ values from DMRG, while solid lines are fits to the free particle $S^z_{\text{free},l}(i_P)$ ($S^z_{\text{tot}} = 8$) and soliton $S^z_{\text{sol},l}(i_P)$ state ($S^z_{\text{tot}} = 1$). Even (odd) refers to the parity of the site. (d) Left: $S = 1/2$ soliton (arrow) breaking short-range dimer order [32]. The shaded rectangles represent singlets, the haze their binding energy. Right: Soliton structure for $H_{c1} < H < H_{c2}$, with $B_{l,p} = 0$ for simplicity. (e) Expected NMR line shape for a soliton lattice. The line symmetric about the zero is for $m_{l,\parallel} = 0$ and $m_{l,\perp} \neq 0$. The solid line used for a comparison with experimental data is for a mean moment $\langle S^z \rangle \neq 0$ and $B_{l,p} = 0.5$.

modeled by the Hamiltonian of two coupled frustrated J_1-J_2 chains, previously suggested for $BiCu_2PO_6$ in Ref. [14] (with $J_1 = J_2$, $\tilde{J}_2 = J_2/2$, $J_\perp = 3J_1/4$, and $J_1/k_B \simeq 140$ K). We considered the limit $H \gtrsim H_{c1}$ in systems with sizes up to $2 \times L$ and $L = 128$. The complete study will be published elsewhere [32]. The main results reported here turn out to be *qualitatively* different from those expected in the classical, the BEC, and the triplon crystallization case. In a standard BEC scenario, for $H \gtrsim H_{c1}$ the local spin projection along the quantization axis $S^z(i)$ (proportional to the boson density n [6]) is uniform, while the transverse spin component (proportional to $\sqrt{n}$) exhibits LRO [6]. In a strictly 1D system of length L, LRO disappears due to quantum fluctuations, while the triplet excitations behave essentially as an ensemble of noninteracting and tightly bound hard-core bosons [8]. We indeed find these features only when n is sufficiently large, e.g., in the $n = S^z_{tot} = 8$ simulation of Fig. 3(c). There, we fit $S^z(i)$ with $S^z_{free,l}(i_P) = A_{l,P} \sum_{k=1}^{n} |\psi_k(i_P)|^2$ [8], where $\psi_k(i_P)$ is the particle-in-box wave function and P is the site parity; i.e., the i_P values are even or odd multiples of $1/2$ and $A_{1,\mathrm{even/odd}} = A_{2,\mathrm{odd/even}}$. In this regime we expect [32,33] a canted IC spin helix, as depicted in Fig. 3(a). As in the simulations, the different magnitude of the $m_\parallel$, $m_\perp$ moments at the two Cu sites (long or red and short or blue arrows) reflects the alternating NNN exchanges. The propagation vector is similar to the one expected from classical arguments, namely, close to the value $q_c = \pi^{-1} \arccos[-J_1/2(J_2 + \tilde{J}_2)] = 0.608 \approx 2/3$ [32,33].

Approaching the critical field from above, n and the overlap between bosons decrease. At an L-dependent value of n, the DMRG results surprisingly show a fractionalization of the FI triplons into two $S = 1/2$ objects. For the $S^z_{tot} = 1$ case in Fig. 3(c), e.g., the sum of the $S^z(i)$ for one leg gives $1/2$. In this new regime, a description of the FI phases in terms of a triplon BEC ceases to be valid. The following DMRG results [32,33] are essential for a comparison with experimental data in this regime. (i) When interacting, the solitons first shrink to the intrinsic width $\xi \ll L$. At this stage, the interactions among solitons affect mainly the soliton-soliton distance but not ξ [34]. Therefore, with increasing field the solitons start to overlap, and at a critical density $n^c_{sol} \approx 1/2\xi$, due to their mutual repulsion, a transition to an IC spin helix occurs at a critical field H_{c2}. The region with FI order and $\mathbf{H} \parallel b$ investigated via NMR in the present work corresponds to $H_{c1} \leq H \leq H_{c2}$. (ii) The driving mechanism for the soliton formation is the frustration-induced tendency to form *short-range* dimer order [35], namely, NNN singlets whose binding energies decay with the distance from the center of the soliton [see the sketch on the left of Fig. 3(d)]. The dimer order is therefore not LR, as in spin-Peierls materials [36] or in frustrated chains ($J_\perp = 0$) [10,11]. To fit the two soliton-in-box shapes of the $S^z_{tot} = 1$ data of Fig. 3(c), we used the expression $S^z_{sol,l}(i_P) = [1 + B_{l,P} \sin(2\pi i q + \theta_{l,P})] S^z_{free,l}(i_P)$, similar to the $J_\perp = 0$ case [11]. However, here q is incommensurate, $\theta_{l,\mathrm{even}} = \theta_{l,\mathrm{odd}} + \pi$, and $B_{1,\mathrm{even/odd}} = B_{2,\mathrm{odd/even}}$. (iii) Because of spin-spin correlations [6], magnetic order is predicted to arise in the spin component transverse to the applied field for $H > H_{c1}$, but a spin helix develops only above the second-order phase transition at $H = H_{c2}$. We suggest that this transition corresponds to the one observed in $BiCu_2PO_6$ at $H_{c2} \simeq 35$ T using the same field orientation [16].

For the comparison with experimental data in the region $H_{c1} \leq H \leq H_{c2}$, we need to describe the solitonic phase in the $L \to \infty$ limit. Because of (i)–(iii), we start from the equation for $\mathbf{S}_{i,l}$ representing the untilted cone (η, $\epsilon = 0$) depicted in Fig. 3(a), which represents the $H > H_{c2}$ regime. For θ_i we *phenomenologically* insert the solution of the sine-Gordon equation with modulus k [37], which is known to model regular patterns of solitons [19,38,39]. From DMRG, $\xi \approx 4$ [33]. If $m_{l,\parallel} = 0$ and $m_{l,\perp} \neq 0$, the calculated spin structure $\mathbf{S}_{i,l}$ exhibits zero magnetization, but the commensurate regions between soliton phase slips cause the predicted NMR profile to exhibit a triple peak [black line in Fig. 3(e)]. This line profile is qualitatively the same as those which were claimed to indicate soliton formation in charge-density-wave materials [19,40]. For $m_{l,\parallel} \neq 0$, we take $m_{l,\parallel}(i_P) = S^z_{sol,l}(i_P)$, replacing $S^z_{free,l}(i_P)$ with the local soliton density $A_{l,P} \nabla_{i_P} \theta[i_P/(k\xi), k]$ [36,37]. On the right of Fig. 3(d) we display, for simplicity with $B_{l,P} = 0$ and for one leg only, one period of the soliton spin structure on which the comparison of our model with the NMR data is based. As $k \to 0$, this structure equals that in Fig. 3(a). The resulting NMR line profile, shown in Fig. 3(e), satisfactorily describes the experimental data, supporting the validity of this description.

In summary, the field-induced order of the frustrated zigzag ladder $Bi(Cu_{1-x}Zn_x)_2PO_6$ has been investigated via ^{31}P NMR with $H||b$. Because of frustration, a hard-core boson description of the FI QPT does not apply in our case. Combined NMR data and DMRG calculations suggest a magnetization process for such systems involving the formation of a soliton lattice. Our model also predicts a *second-order* transition at H_{c2} [32] which, most likely, corresponds to the one observed in recent experiments [16]. For $\mathbf{H} \nparallel b$, the $\mathbf{g}$ tensor and the rung-DM anisotropy are more influential and, therefore, will have to be included to model the complexity of the overall phase diagram [16].

The authors thank T. Giamarchi, P. Bouillot (Uni-Geneva), M. Troyer (ETHZ), and C. Batista (LANL) for numerous illuminating discussions. We thank A. A. Tsirlin (MPI) for sharing his data prior to publication. We acknowledge the EC support via the 7th framework program "Transnational Access," Contract No. 228043-EuroMagNET II-Integrated Activities. This work was

financially supported also by the Schweizerische Nationalfonds zur Förderung der Wissenschaftlichen Forschung (SNF), the NCCR research pool MaNEP of SNF, and the NSF Grant No. DMR-0955707.

*fcasola@phys.ethz.ch

[1] T. Matsubara and H. Matsuda, Prog. Theor. Phys. **16**, 569 (1956)

[2] T. Giamarchi, Ch. Rüegg, and O. Tchernyshyov, Nat. Phys. **4**, 198 (2008).

[3] M. Takigawa and F. Mila, in *Introduction to Frustrated Magnetism*, edited by C. Lacroix, P. Mendels, and F. Mila (Springer, New York, 2011), p. 241.

[4] K. Kodama, M. Takigawa, M. Horvatić, C. Berthier, H. Kageyama, Y. Ueda, S. Miyahara, F. Becca, and F. Mila, Science **298**, 395 (2002).

[5] E. G. Batyev and L. S. Braginskii, Sov. Phys. JETP **60**, 781 (1984); I. Affleck, Phys. Rev. B **41**, 6697 (1990).

[6] T. Giamarchi and A. M. Tsvelik, Phys. Rev. B **59**, 11398 (1999).

[7] V. S. Zapf, D. Zocco, B. R. Hansen, M. Jaime, N. Harrison, C. D. Batista, M. Kenzelmann, C. Niedermayer, A. Lacerda, and A. Paduan-Filho, Phys. Rev. Lett. **96**, 077204 (2006); S. Krämer, R. Stern, M. Horvatić, C. Berthier, T. Kimura, and I. R. Fisher, Phys. Rev. B **76**, 100406(R) (2007); S. E. Sebastian, N. Harrison, C. D. Batista, L. Balicas, M. Jaime, P. A. Sharma, N. Kawashima, and I. R. Fisher, Nature (London) **441**, 617 (2006); Ch. Rüegg, N. Cavadini, A. Furrer, H.-U. Güdel, K. Krämer, H. Mutka, A. Wildes, K. Habicht, and P. Vorderwisch, Nature (London) **423**, 62 (2003).

[8] J.-B. Fouet, F. Mila, D. Clarke, H. Youk, O. Tchernyshyov, P. Fendley, and R. M. Noack, Phys. Rev. B **73**, 214405 (2006).

[9] T. Nikuni and H. Shiba, J. Phys. Soc. Jpn. **64**, 3471 (1995).

[10] B. S. Shastry and B. Sutherland, Phys. Rev. Lett. **47**, 964 (1981); D. Khomskii, W. Geertsma, and M. Mostovoy, Czech. J. Phys. **46**, 3239 (1996).

[11] E. Sørensen, I. Affleck, D. Augier, and D. Poilblanc, Phys. Rev. B **58**, R14701 (1998).

[12] B. Koteswararao, S. Salunke, A. V. Mahajan, I. Dasgupta, and J. Bobroff, Phys. Rev. B **76**, 052402 (2007).

[13] S. Wang, E. Pomjakushina, T. Shiroka, G. Deng, N. Nikseresht, Ch. Rüegg, H.-M. Rønnow, and K. Conder, J. Cryst. Growth **313**, 51 (2010).

[14] A. A. Tsirlin, I. Rousochatzakis, D. Kasinathan, O. Janson, R. Nath, F. Weickert, C. Geibel, A. M. Läuchli, and H. Rosner, Phys. Rev. B **82**, 144426 (2010).

[15] O. Mentré, E. Janod, P. Rabu, M. Hennion, F. Leclercq-Hugeux, J. Kang, C. Lee, M.-H. Whangbo, and S. Petit, Phys. Rev. B **80**, 180413 (2009).

[16] Y. Kohama, S. Wang, A. Uchida, K. Prša, S. Zvyagin, Y. Skourski, R. D. McDonald, L. Balicas, H. M. Rønnow, Ch. Rüegg, and M. Jaime, Phys. Rev. Lett. **109**, 167204 (2012).

[17] The actual Zn content, measurable directly via NMR [18], is found to be $x = 0.0081(5)$ for the sample investigated.

[18] F. Casola, T. Shiroka, S. Wang, K. Conder, E. Pomjakushina, J. Mesot, and H.-R. Ott, Phys. Rev. Lett. **105**, 067203 (2010).

[19] R. Blinc, Phys. Rep. **79**, 331 (1981).

[20] F. Casola *et al.* (unpublished).

[21] By definition $M_1 = \int_{-\infty}^{+\infty} fI(f)df = \gamma_P N^{-1} \sum_{p,j} h_p(j)$ and $W = \sqrt{M_2} = [\int_{-\infty}^{+\infty} (f - M_1)^2 I(f) df]^{1/2} = [\gamma_P^2 N^{-1} \times \sum_{p,j} h_p^2(j) - M_1^2]^{1/2}$, with N the total number of j sites.

[22] N. Fujiwara, T. Goto, S. Maegawa, and T. Kohmoto, Phys. Rev. B **47**, 11860 (1993).

[23] R. Yu, S. Haas, and T. Roscilde, Europhys. Lett. **89**, 10009 (2010).

[24] S. Wang *et al.* (unpublished).

[25] V. O. Garlea, A. Zheludev, K. Habicht, M. Meissner, B. Grenier, L.-P. Regnault, and E. Ressouche, Phys. Rev. B **79**, 060404(R) (2009).

[26] S. Miyahara, J.-B. Fouet, S. R. Manmana, R. M. Noack, H. Mayaffre, I. Sheikin, C. Berthier, and F. Mila, Phys. Rev. B **75**, 184402 (2007).

[27] T. Nikuni, M. Oshikawa, A. Oosawa, and H. Tanaka, Phys. Rev. Lett. **84**, 5868 (2000).

[28] E. Wulf, S. Mühlbauer, T. Yankova, and A. Zheludev, Phys. Rev. B **84**, 174414 (2011).

[29] V. Kiryukhin, B. Keimer, J. P. Hill, S. M. Coad, and D. McK. Paul, Phys. Rev. B **54**, 7269 (1996).

[30] R. Bursill, G. A Gehring, D. J. J. Farnell, J. B. Parkinson, T. Xian, and C. Zengt, J. Phys. Condens. Matter **7**, 8605 (1995).

[31] M. Enderle, C. Mukherjee, B. Fåk, R. K. Kremer, J.-M. Broto, H. Rosner, S.-L. Drechsler, J. Richter, J. Malek, A. Prokofiev, W. Assmus, S. Pujol, J.-L. Raggazzoni, H. Rakoto, M. Rheinstædter, and H. M. Rønnow, Europhys. Lett. **70**, 237 (2005).

[32] A. Feiguin *et al.* (unpublished).

[33] For more information about the DMRG analysis, see F. Casola *et al.*, arXiv:1211.5522.

[34] J. Zang, S. Chakravarty, and A. R. Bishop, Phys. Rev. B **55**, R14705 (1997).

[35] A. Lavarélo, G. Roux, and N. Laflorencie, Phys. Rev. B **84**, 144407 (2011).

[36] H. M. Rønnow, M. Enderle, D. F. McMorrow, L.-P. Regnault, G. Dhalenne, A. Revcolevschi, A. Hoser, K. Prokes, P. Vorderwisch, and H. Schneider, Phys. Rev. Lett. **84**, 4469 (2000); M. Horvatić, Y. Fagot-Revurat, C. Berthier, G. Dhalenne, and A. Revcolevschi, Phys. Rev. Lett. **83**, 420 (1999).

[37] M. Abramowitz and I. Stegun, *Handbook of Mathematical Functions* (Dover, New York, 1972), Chap. 16, pp. 567–581.

[38] A. R. Bishop, Phys. Scr. **20**, 409 (1979).

[39] K. Maki and P. Kumar, Phys. Rev. B **14**, 118 (1976).

[40] D. Koumoulis, N. Panopoulos, A. Reyes, M. Fardis, M. Pissas, A. Douvalis, T. Bakas, D. N. Argyriou, and G. Papavassiliou, Phys. Rev. Lett. **104**, 077204 (2010).